Rare dermatomuscular manifestations in a patient with small lymphocytic lymphoma: A case report

YUNG-LUN CHOU[1], TZU-CHUAN HUANG[2], YUAN-YUEI CHEN[3] and SHIUE-WEI LAI[2]

[1]Department of Family and Community Medicine, Tri-Service General Hospital, National Defense Medical Center, Taipei 11490, Taiwan, R.O.C.; [2]Division of Hematology/Oncology, Department of Internal Medicine, Tri-Service General Hospital, National Defense Medical Center, Taipei 114202, Taiwan, R.O.C.; [3]Department of Pathology, Tri-Service General Hospital, National Defense Medical Center, Taipei 114202, Taiwan, R.O.C.

Received May 16, 2023; Accepted October 31, 2024

DOI: 10.3892/etm.2025.12904

Abstract. Small lymphocytic lymphoma is generally considered one of the indolent non-Hodgkin lymphoma with slow progression. However, in certain cases of small lymphocytic lymphoma (SLL), an atypical clinical presentation may be observed, such as musculocutaneous involvement, which needs to be differentiated from uncontrollable cellulitis or dermatitis. Compared with T-cell leukemia/lymphoma, cutaneous lesions in patients with SLL are far less common. The current study presented a rare case of SLL with an unusual clinical manifestation, rapid disease progression and therapeutic response after a systemic therapy regimen was applied.

Introduction

Chronic lymphocytic leukemia (CLL) and small lymphocytic lymphoma (SLL) are different manifestations of a mature B-cell neoplasm with a progressive accumulation of monoclonal B lymphocytes. CLL accounts for ~25-35 and 10% of all cases of leukemia in the United States and Asian countries, respectively (1,2). The incidence rate of SLL is remarkably low in Asia and compared with patients with CLL/SLL in Western countries, Asian patients with CLL/SLL are younger and have an adverse prognosis (3). Compared with other types of leukemia or lymphoma, cutaneous infiltration by malignant leukocytes is far less common in patients with CLL/SLL (4). The current study reported a rare case of SLL with cutaneous and musculotendinous involvement in the left lower extremity as the initial symptom.

Correspondence to: Dr Shiue-Wei Lai, Division of Hematology/Oncology, Department of Internal Medicine, Tri-Service General Hospital, National Defense Medical Center, 325, Sec. 2 Chenggong Road, Neihu, Taipei 114202, Taiwan, R.O.C.
E-mail: xsurferlai@gmail.com

Key words: small lymphocytic lymphoma, chronic lymphocytic leukemia, lymphoma cutis, rituximab

Case report

A 65-year-old Asian man with chronic hepatitis B virus infection presented with left calf and ankle pain along with swelling and erythema lasting for 2 months. Although the patient was treated for presumed cellulitis with empiric antibiotics, no clinical improvement was observed. The patient arrived at the emergency room of the Tri-Service General Hospital (Taipei, Taiwan) with symptoms of progressive painful swelling and difficulty walking in October 2021. On examination, erythematous changes over the left ankle and calf along with tenderness were observed (Fig. 1). Homan's sign of the left lower extremity was negative and the results of initial biochemical tests were inconclusive, except for mild bicytopenia and elevation of C-reactive protein levels. The hemoglobin level was 8.2 g/dl (reference range: 13.5-17.5 g/dl in adult males), the mean corpuscular volume was 80.4 fl (reference range: 80-100 fl in adults) and the platelet count was $145x10^3/\mu l$ (reference range: $150\text{-}350x10^3/\mu l$ in adults). The serum C-reactive protein level was 0.83 mg/dl (reference range: >0.3 mg/dl in adults). There was no leukocytosis or lymphocytosis. The total white blood cell count was $6.78x10^3/\mu l$ (reference range: $4.5\text{-}11x10^3/\mu l$ in adults), the absolute neutrophil count was $2.12x10^3/\mu l$. (reference range: $1.8\text{-}7.7x10^3/\mu l$ in adults) and the absolute lymphocyte count was $3.02x10^3/\mu l$ (reference range: $1.5\text{-}4x10^3/\mu l$ in adults). Abdominal computed tomography (CT) revealed multiple paraaortic, iliac and inguinal lymphadenopathy (Fig. 2). Therefore, an excisional biopsy of the left inguinal region was performed in November 2021 and the histopathological report revealed B-cell lymphoma characterized by lymphoid structure effacement with monotonous small-sized hyperchromatic malignant cells. Protocols are provided in Data S1 and the protocols of IHC for the same markers are the same over different tissue (lymph node, bone marrow and skin). Immunohistochemical (IHC) staining results (positive for CD5, CD20, CD23, Bcl-2, CD79a and negative for cyclin D1 for malignant cells) indicated CLL/SLL (Figs. 3 and S1). The degree of small round lymphocyte infiltration in the lymph node was ~90%. In addition, after fasting for 6 h, the patient underwent 18-fluorodeoxyglucose positron emission tomography/computed tomography (^{18}F-FDG PET/CT) in November 2021 (protocol provided in Data S2, which revealed

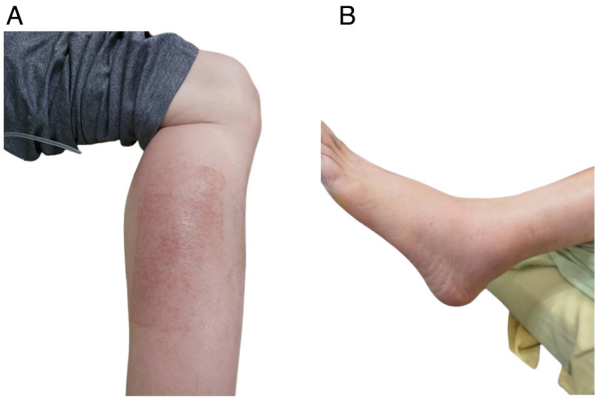

Figure 1. Inspection of left lower extremity. (A) The left calf during the initial presentation. (B) The left ankle during the initial presentation.

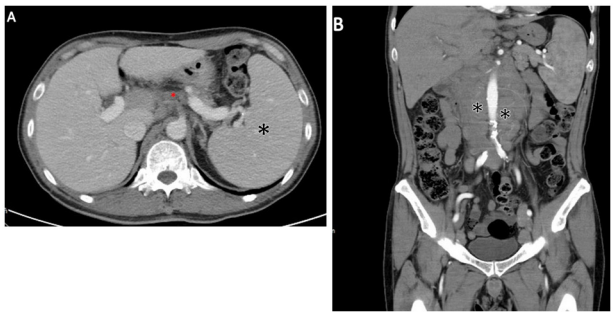

Figure 2. Initial abdominal CT. Dynamic CT images were obtained during non-enhanced and portal venous phase scan following intravenous contrast injection. Confluent enlarged lymph nodes over the gastrohepatic ligament, hepatoduodenal ligament, aorto-caval region, bilateral iliac chains and inguinal regions are visible. (A) In the aortic phase of the axial view, para-aortic lymphadenopathies were observed (red asterisk). Splenomegaly was also present (black asterisk). (B) In the aortic phase of the coronal view, mesenteric lymphadenopathies may be observed (black asterisks). CT, computed tomography.

multiple low-grade fluorodeoxyglucose uptake nodules over several lymphatic sites, including gastrohepatic and hepatoduodenal ligaments, para-aortocaval spaces and bilateral iliac chains, except for the skin and musculoskeletal system (Fig. 4). Histology of a bone marrow biopsy (November 2021) indicated a homogenous population of small lymphocytes infiltrating the myeloid tissue. The IHC staining results (malignant cells positive for CD5, CD20, CD23, CD43, CD79a and Bcl-2) were in favor of a prognosis of CLL/SLL (Fig. 5). The degree of small round lymphocyte infiltration in the bone marrow was ~70%. According to the International Workshop on CLL guidelines (5), the definition of SLL requires the presence of lymphadenopathy and the absence of cytopenias caused by a clonal marrow infiltrate. In addition, the number of B lymphocytes in the peripheral blood should be $<5x10^9$/l. In SLL, the diagnosis should be confirmed by histopathological evaluation of a lymph node biopsy or biopsy of other tissues. A diagnosis of SLL in Lugano stage IV, with multiple lymphadenopathies and bone marrow infiltration, was established and fluorescence *in situ* hybridization analysis of the short arm of chromosome 17 (6) revealed no deletions (the FISH panels including the probes for 11q22.3 (ATM), 17p13.1 (Tp53), 12p11.1-q11 (CEP 12), 13q34, 13q14.3 (LSI D13S319) were all from Vysis, Inc. Based on the MABLE study (7) and the reimbursement of the National Health Insurance (NHI), the patient received one treatment course of chemoimmunotherapy with rituximab and bendamustine (RB) in November 2021. The RB regimen was as follows: Rituximab 375 mg/m^2 intravenously (IV) on day 1, plus RB 90 mg/m^2 IV on days 1 and 2. Although the patient's cutaneous symptoms on the left calf and ankle improved in the following two weeks, new erythematous skin changes developed over the dorsal side of the left internal thigh two months later from initial encounter (Fig. 6).

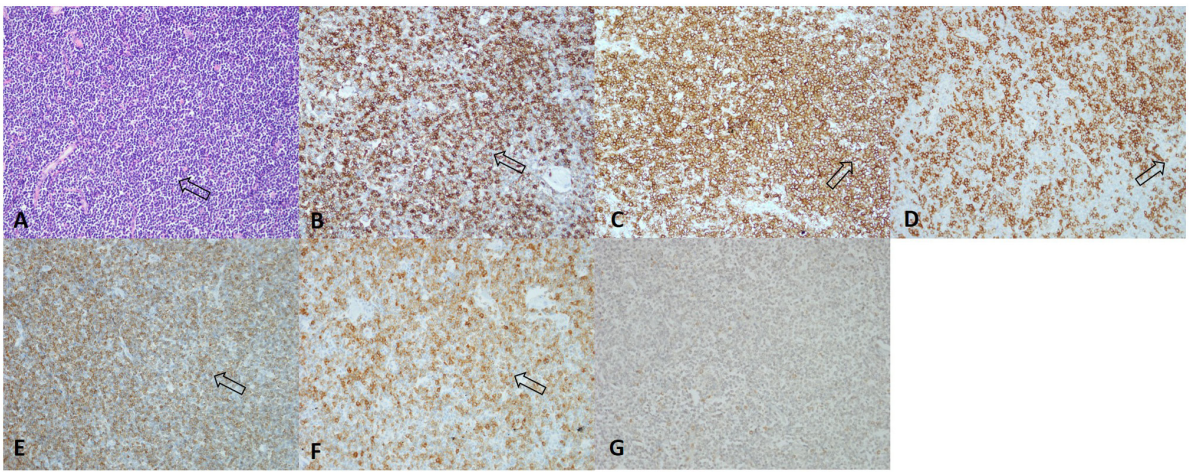

Figure 3. Microscopic examination of left inguinal lymph node biopsy specimen. (A) Histology showed effacement of lymphoid structure with monotonous small-sized hyperchromatic malignant cells. The majority of the malignant cells are small round lymphocytes (black arrow) and the severity of infiltration was ~90% (H&E stain). (B) IHC stain for CD5 revealed positive staining of malignant cells. Brown coloration (black arrow) represents positive CD5 staining. (C) IHC stain for CD20 revealed positive staining of malignant cells. Brown coloration (black arrow) represents positive CD20 staining. (D) IHC stain for CD23 revealed positive staining of malignant cells. Brown coloration (black arrow) represents positive CD23 staining. (E) IHC stain for Bcl-2 revealed positive staining of malignant cells. Brown coloration (black arrow) represents positive Bcl-2 staining. (F) IHC stain for CD79a revealed positive staining of malignant cells. Brown coloration (black arrow) represents positive CD79a staining (G) IHC stain for Cyclin D1 revealed negative staining of malignant cells (magnification, x200). IHC, immunohistochemistry.

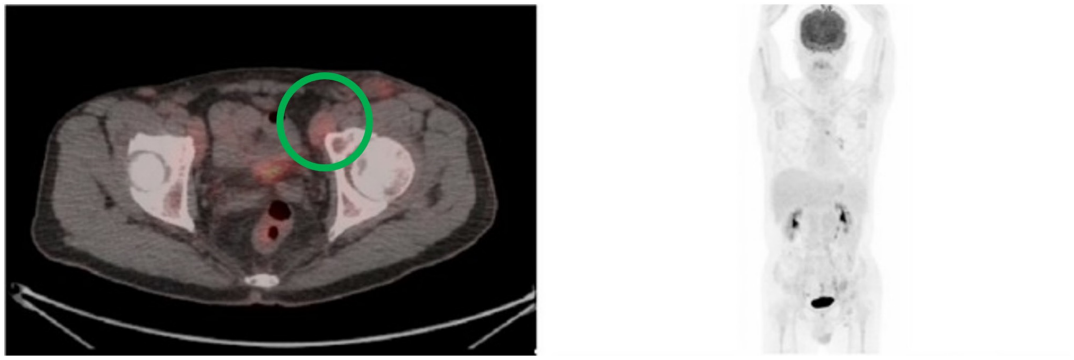

Figure 4. Whole-body FDG PET/CT scan. Initial PET/CT scan showed multiple low-grade FDG-avid nodules over several lymphatic sites on both sides of the diaphragm, with the most intense FDG avidity being over the left internal iliac chain. The left panel shows an axial view at the hip level of the PET/CT. The red coloration indicates high radiotracer uptake, such as active metabolic processes (malignancy or inflammation). The right panel shows a coronal view of the MIP PET image. The green circle indicates the most intense FDG avidity (with a maximal standardized uptake value of ~6.6 at the left internal iliac chain). PET-CT, positron emission tomography-computed tomography; FDG, 18-fluorodeoxyglucose; ROI, region of interest; MIP, maximum intensity projection.

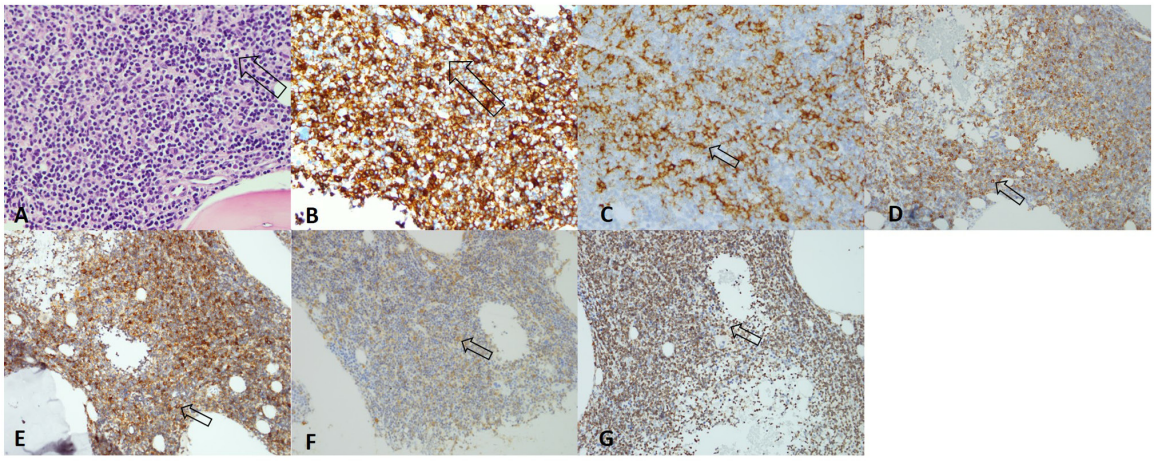

Figure 5. Microscopic examination of bone marrow biopsy specimen. (A) On histology, a homogeneous population of small infiltrating lymphocytes was observed in the myeloid tissue. The majority of the malignant cells were small round lymphocytes (black arrow) and the degree of infiltration was ~70% (H&E staining). (B) IHC stain for CD5 revealed positive staining of malignant cells. Brown coloration (black arrow) represents positive CD5 staining (C) IHC stain for CD20 revealed positive staining of malignant cells. Brown coloration (black arrow) represents positive CD20 staining. (D) IHC stain for CD23 reveals positive staining of malignant cells. Brown coloration (black arrow) represents positive CD23 staining. (E) IHC staining for CD43 reveals positive staining of malignant cells. Brown coloration (black arrow) represents positive CD43 staining. (F) IHC stain for CD79a reveals positive staining of malignant cells. Brown coloration (black arrow) represents positive CD79a staining. (G) IHC stain for Bcl-2 revealed positive staining of malignant cells. Brown coloration (black arrow) represents positive Bcl-2 staining (magnification, x200). IHC, immunohistochemistry.

Ultrasonography of the left posterior thigh in December 2021 demonstrated target-like lesions over semimembranosus muscles and tendons with a hypoechoic rim and hyperechoic core (Fig. 7). Examination of a skin biopsy of the lesion site in December 2021 revealed atypical small lymphocytes with perivascular infiltration of the skin dermis. The severity of atypical small lymphocyte infiltration in the dermal layer was ~50%. In addition, the results of IHC staining were positivity of reactive T cells for CD3 (Fig. 8C), as well as positivity of malignant cells (the abnormal lymphocytes that exhibit staining are the malignant cells) for CD5 (Fig. 8D) but negativity for CD3 (Fig. 8C) and CD20 (Fig. 8E). According to the patient's medical records and IHC results, this finding was consistent with lymphoma cutis, with suspected semimembranosus involvement. The patient had received two cycles of the RB regimen (November and December 2021) and the regimen was switched to R-CHOP (rituximab, cyclophosphamide,

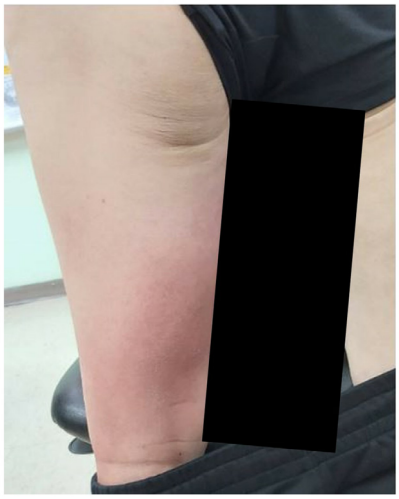

Figure 6. Inspection of the left internal thigh two months after the initial encounter.

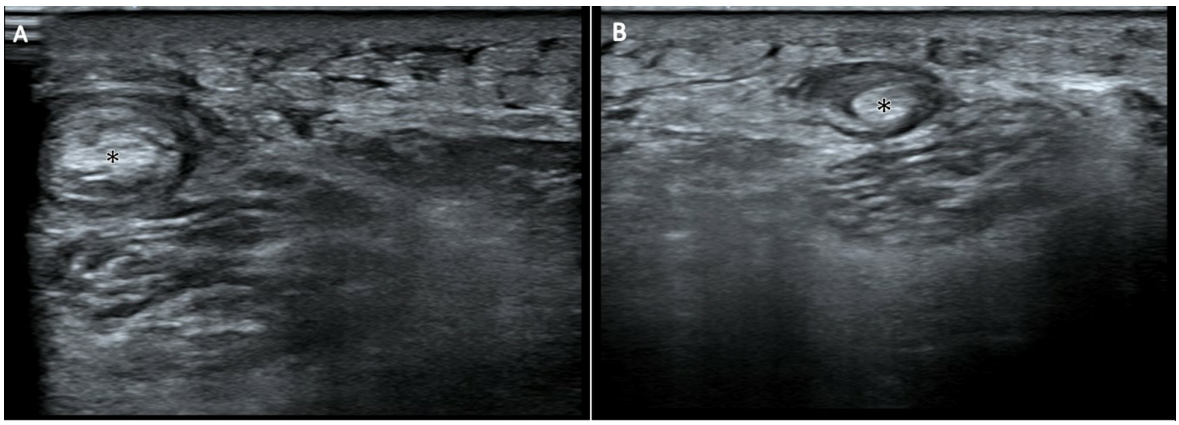

Figure 7. Ultrasonography of the left posterior thigh. (A) Convex array real-time sonography for the subcutaneous layer of the posterior aspect of the left thigh reveals the target appearance with hypoechoic rim and hyperechoic core (black asterisk) over the semimembranosus. (B) In the popliteal fossa of the left knee, there is also a target appearance with hypoechoic rim and hyperechoic core (black asterisk) over the semimembranosus.

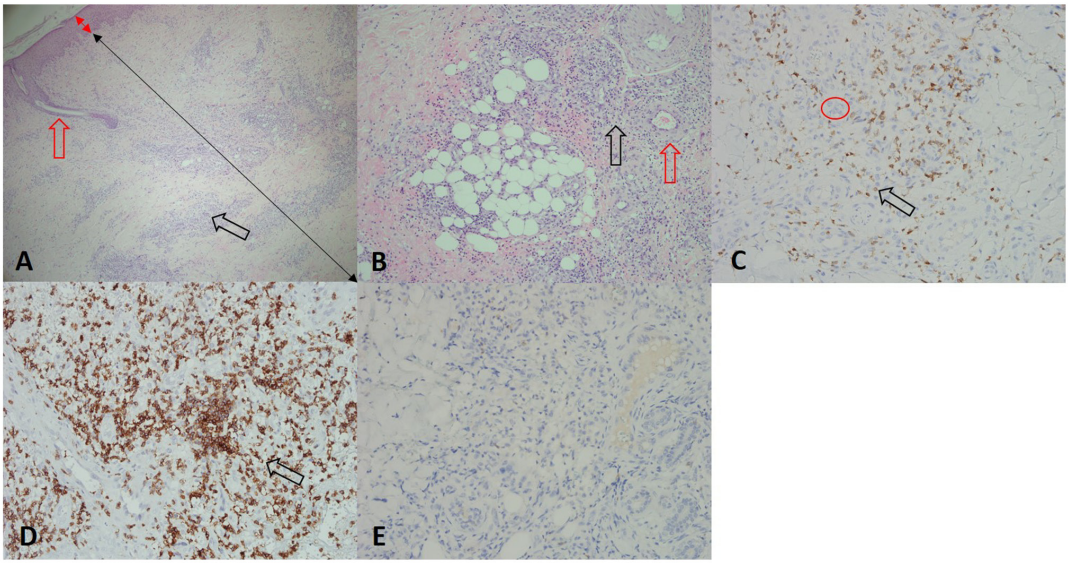

Figure 8. Microscopic examination of the cutaneous biopsy of the left internal thigh. (A) Histology indicates atypical small lymphocyte infiltration of the skin dermis. The degree of infiltration is ~50% (red double-headed arrow: Epidermis; black double-headed arrow: Dermis; red arrow: Hair follicle; black arrow: Abnormal small lymphocytes) (H&E stain; magnification, x40). (B) Histology at a greater magnification indicated atypical small lymphocytes with perivascular infiltration of the skin dermis (black arrow: Atypical small lymphocytes; red arrow: Perivascular infiltration) (H&E stain). (C) IHC stain for CD3 revealed positive staining of reactive T cells (black arrow) but negative staining of abnormal lymphocytes (red circle). (D) IHC stain for CD5 revealed positive staining of abnormal lymphocytes. Brown coloration (black arrow) represents positive CD5 staining. (E) IHC stain for CD20 revealed negative staining. None of the brown coloration of the cells was identified from this slice (magnification, x200). IHC, immunohistochemistry.

doxorubicin, vincristine and prednisolone) in January 2022 under reimbursement in Taiwan because of the inadequate treatment response and the unaffordability of the Bruton's tyrosine kinase inhibitor (BTKi) combination (the BTKi used in CLL/SLL includes ibrutinib, acalabrutinib and zanubrutinib) at that time. The dosages of R-CHOP included intravenous infusion of rituximab (375 mg/m^2) on day 1, cyclophosphamide (750 mg/m^2) on day 1, doxorubicin (50 mg/m^2) on day 1, vincristine (1.4 mg/m^2) on day 1 and oral prednisone (40 mg/m^2) on days 1 to 5, for every three weeks per cycle (R-CHOP is typically given in about six cycles and each cycle is spaced three weeks apart). The patient's symptoms gradually improved after three consecutive treatment courses. The follow-up ^{18}F-FDG PET/CT 4.5 months after the initial encounter for the evaluation of treatment response revealed a stable disease status compared with the initial scan, without any evidence of substantially abnormal FDG uptake (Fig. 9). Considering the possible significant adverse events of chemotherapy, including myelosuppression, nausea and fatigue, after 6 cycles of R-CHOP, ibrutinib was administered at the patient's own expense and rituximab infusion until the supply of rituximab for reimbursement was exhausted in January 2024 (8). Ibrutinib was also discontinued at that month due to its cost. The patient underwent a whole-body PET scan in January 2024 (Fig. 10A). Compared to the previous scan from August 2023 [little interval change with moderate FDG-avidity over several lymph nodes involving the para-vascular [maximal standardized uptake value (SUVmax)=4.7], right lower paratracheal (SUVmax=4.4), left-sided paraaortic (SUVmax=6.3) and

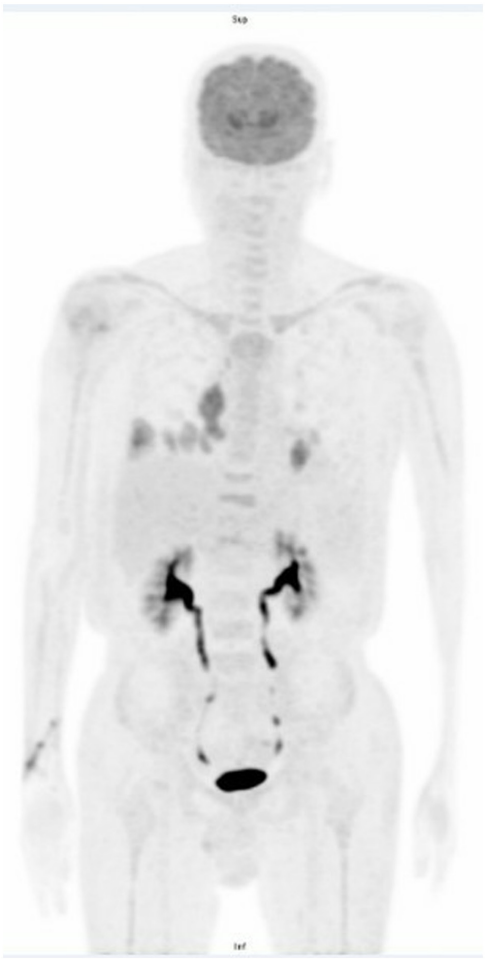

Figure 9. Later PET scan (4.5 months after first encounter) revealed a certain ill-defined FDG avidity over the lower bilateral lobes of the lungs, corresponding to patchy consolidation and focal atelectasis. However, no evidence of substantially abnormal FDG uptake was found. PET, positron emission tomography; FDG, 18-fluorodeoxyglucose.

RLL nodule (SUVmax=5.0), suspicious residual malignancy in stable status], which revealed residual malignancy in a stable state [Deauville (9) score, 4], the current imaging results may indicate lymphoma, likely accompanied by inflammation, affecting the mediastinum, right lower lobe of the lung and skin on the left buttock, with the patient remaining in a relatively stable condition during treatment. In September 2024, the patient had another whole-body PET scan (Fig. 10B). When compared to the FDG PET/CT from January 2024, the latest imaging findings again suggested lymphoma, possibly mixed with inflammation, involving the same areas post-treatment in a relatively stable disease condition (Deauville score, 3-4). The patient remains in a relatively stable cutaneous condition with regular medical follow-up at three-month intervals without any disease-specific therapy at the outpatient department.

Discussion

Review of the literature indicated that dermatomuscular manifestations of CLL/SLL are uncommon and may be accompanied by various types of skin reactions, including papule, nodule, patch, plaque or ulcerative lesion (10). The most common sites of skin involvement are the head and neck rather than the trunk or extremities (11). Patients with these conditions are considered to be at an increased risk of secondary cutaneous malignancies, such as squamous cell carcinoma (12). The majority of cases with skeletal muscle involvement are mostly diagnosed with diffuse large B-cell lymphoma (13). The patient of the current study presented with recurrent painful swelling and erythema over the left extremity, which raised the suspicion of malignancy and was confirmed by the histopathological report. This clinical manifestation of leukemia/lymphoma originating from a B-cell lineage, which mimicked recurrent cellulitis, increased the difficulty of early diagnosis and delayed the standard therapy.

IHC staining of the left inguinal lymph node biopsy revealed positivity of malignant cells for CD5, CD20, CD23, Bcl-2 and CD79a and negativity for cyclin D1. IHC analysis of the bone marrow aspirate indicated positive staining of malignant cells for CD5, CD20, CD23, CD43, CD79a and Bcl-2. It was possible to differentiate the origin of B cells of CLL/SLL from the other possible B-cell lineage lymphoma (14). Histological analysis of the skin biopsy by H&E staining indicated infiltration of abnormal hyperchromatic cells. After IHC processing, positive CD5 staining of malignant cells, along with negative CD3 and CD20 staining of malignant cells, were noted. Based on the previous therapeutic course, which included rituximab infusion, the likely diagnosis was SLL with infiltration of the dermal layer of the left thigh.

Cyclin D1 serves as a valuable marker for differentiating mantle cell lymphoma (MCL) from other small B-cell lymphomas, as MCL typically expresses high levels of cyclin D1. Most tumors also exhibit CD19, CD20 and moderately high levels of surface immunoglobulin (Ig) (usually IgM and IgD, with either κ or λ light chains). MCL is generally CD5-positive and CD23-negative, which aids in distinguishing it from CLL and SLL. The diagnosis of MCL is usually confirmed through a biopsy of lymph nodes, tissue and bone marrow, revealing the characteristic morphology of monomorphic small- to medium-sized lymphoid cells with irregular nuclear contours. The hallmark chromosomal translocation t(11;14)(q13;q32) is present in most cases of MCL and is responsible for the abnormal expression of cyclin D1, which is not typically found in normal lymphocytes. Immunohistochemistry can detect cyclin D1 in ~98% of MCL cases (15).

The left inguinal lymph node biopsy specimen exhibited IHC staining for cyclin D1 and accordingly, mantle cell lymphoma was less considered. In addition, the IHC staining of lymph node and bone marrow specimens both demonstrated small, atypical lymphocytes with positive staining for CD5 and CD23, which excluded mantle-cell lymphoma, marginal zone lymphoma and large B-cell lymphoma. Besides, lymphoplasmacytic lymphoma (LPL) and SLL are both characteristic of abnormal small lymphocytes on H&E staining. The typical IHC staining result of malignant cells of LPL may be negative for CD5 but positive for CD138 on the IHC stain. The clinical presentation of patients with LPL is varied and can present with symptoms related to tumor infiltration (lymphadenopathy, organomegaly, cytopenias) or monoclonal protein production (hyperviscosity, neuropathy). The pathology of

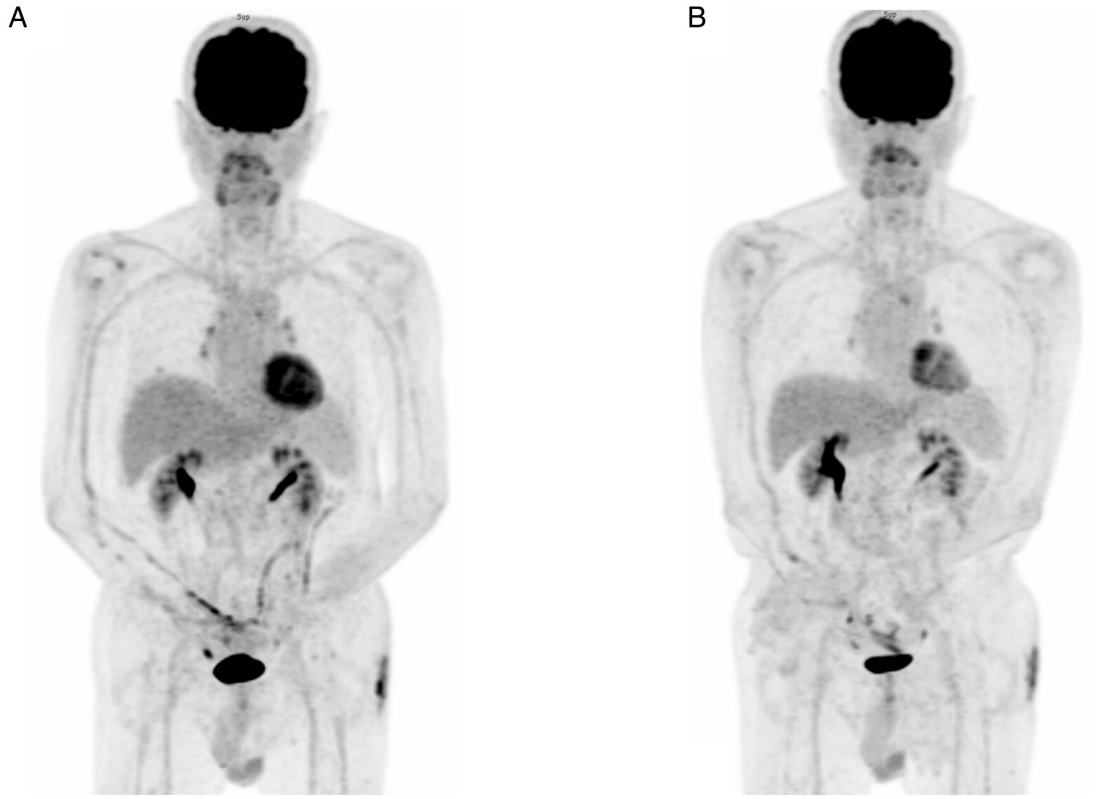

Figure 10. Follow-up PET scans. (A) PET scan in January 2024 (about two years and three months after the first encounter). Relatively stable appearance of the previously noted FDG-avid lesions over the mediastinum (e.g. AP window LN, SUVmax: 4.1), RLL lung (SUVmax: 2.5) and cutaneous region of the left buttock (SUVmax: 7.2), suggesting lymphoma (probably mixed with inflammation) under treatment in a relatively stable disease condition (SD; Deauville score, 4). Furthermore, normal physiological FDG accumulation in the cerebral cortex, adenoids of tonsils, vocal cords, heart, aorta, T-L spines, renal pelves, ureters and bladder was seen. (B) PET scan in September 2024 (about two years and eleven months later after first encounter). The study showed a relatively stable appearance of the previously noted FDG-avid lesions over the mediastinum (e.g. AP LN, SUVmax: 3.8; previously 4.1), RLL lung (SUVmax: 1.6; previously 2.5) and cutaneous region of the left buttock (SUVmax: 4.8; previously 7.2), suggesting lymphoma (probably mixed with inflammation) post-treatment in a relatively stable disease condition (SD; Deauville score, 3-4). Furthermore, normal physiological FDG accumulation in the cerebral cortex, adenoids of tonsils, vocal cords, heart, aorta, T-L spines, renal pelves, ureters and bladder was seen. PET, positron emission tomography; FDG, 18-fluorodeoxyglucose; RLL, right lower lobe; SD, stable disease; AP window, aortopulmonary window; LN, lymph node; SUVmax, maximal standardized uptake value.

LPL is typically composed of small B cells, plasmacytoid lymphocytes and plasma cells involving the bone marrow. The above findings were inconsistent with the pathological IHC staining for the present case. As there was no peripheral blood lymphocytosis, the diagnosis was SLL rather than CLL. The diagnosis of CLL requires the presence of at least $5x10^9$/l B lymphocytes in the peripheral blood. Confirmation of the clonality of these B lymphocytes is achieved by demonstrating Ig light chain restriction through flow cytometry. However, numerous cases of SLL do not exhibit B lymphocytosis and flow cytometry is not typically part of the diagnostic criteria for this disease. In addition, our hospital does not routinely provide access to flow cytometry or Ig heavy chain variable assessments. For the patient of the present study, the musculotendinous involvement of lymphoma over the left posterior thigh was suspected according to the clinical images and the patient refused muscle biopsy due to the invasiveness of this procedure.

Currently, the Lugano classification is used for lymphoma staging with the aid of a PET/CT scan, which was derived from the Ann Arbor staging system (16). The patient was staged using the Lugano classification instead of the Ann Arbor staging system because PET-CT is effective for assessing response in FDG-avid histology using a 5-point scale, while CT is preferred for cases with low or variable FDG avidity, particularly when aggressive transformation is suspected (16). SLL with Lugano stage IV was finally confirmed because the lymphoma involved multiple lymph nodes and bone marrow, without peripheral blood lymphocytosis.

According to the National Comprehensive Cancer Network guidelines for CLL/SLL, the preferred therapeutic regimens for CLL/SLL without del(17p)/TP53 mutation include BTKi with/without anti-CD20 monoclonal antibodies, venetoclax with obinutuzumab or (chemo) immunotherapy (17). BTKi and venetoclax are not covered under the reimbursement policies of the NHI in Taiwan based on the patient's diagnosis and clinical condition. After discussion with the patient and his family about therapeutic effects, possible adverse events and the cost-effectiveness, they opted for ibrutinib at their personal expense and rituximab infusion until the reimbursed supply of rituximab was exhausted. The initial choice of the RB regimen for the patient was based on the MABLE study (7) and the reimbursement policies of the NHI. In addition, SLL is typically classified as an indolent lymphoma, which is why the treatment strategy did not initially include the R-CHOP regimen, as this is primarily indicated for more aggressive non-Hodgkin's lymphomas, such as diffuse large B-cell

lymphoma or advanced follicular lymphoma. The patient received two cycles of the RB regimen in late November and late December 2021. However, due to an inadequate treatment response, extranodal involvement and the high cost of BTKi, the regimen was switched to R-CHOP in late January 2022 under NHI reimbursement.

Concerning the skin biopsy results of the left thigh, the IHC staining results were positive for CD5 but negative for CD23 and CD20. In terms of the phenotypic changes of IHC staining of CD20-positive B-cell lymphoma, Maeshima *et al* (18) observed that after rituximab-containing chemotherapies, CD20 protein-negative or -decreased phenotypic changes were confirmed in 5 cases among 36 patients when the disease progressed. Until a CD20-negative phenotypic change occurred, 4 to 14 cycles of rituximab were administered and the duration of relapse or progression from their first treatment with rituximab ranged from 2 to 81 months. There is no exact duration from initiation of rituximab-containing therapy to CD20-negative transformation due to the rarity of this population. Of note, due to IHC staining results of CD20 changing after rituximab therapy (one of the chimeric monoclonal antibodies targeted against CD20), which is one of the major mechanisms of treatment resistance in non-Hodgkin B cell lymphomas (19), clinicians are required to follow up the treatment responses closely and switch the regimen in a timely manner. A limitation of the present study is that IHC co-staining could not be performed at our laboratory due to the lack of applicable antibodies, which was an obstacle for differential diagnosis.

In summary, due to the diverse etiologies of dermatomuscular manifestations, it is crucial to actively monitor treatment responses. The potential for malignancy should always be included in the differential diagnoses. In addition, in newly diagnosed cases of SLL, thorough investigation of skin changes or symptoms is essential for accurate clinical staging and selection of appropriate treatment regimens.

Acknowledgements

Not applicable.

Funding

No funding was received.

Availability of data and materials

The data generated in the present study may be requested from the corresponding author.

Authors' contributions

YLC drafted the manuscript. SWL conceptualized and designed the study. YYC processed the H&E and IHC staining of the tissue specimens and provided the interpretation for pathological results. YLC, SWL and YYC collected clinical information and performed the analysis. TCH, YYC and SWL interpreted the data and critically reviewed and revised the manuscript. YLC and SWL confirmed the authenticity of all the raw data. All authors have read and approved the final manuscript.

Ethics approval and consent to participate

The present study was approved by the Institutional Review Board of the Tri-Service General Hospital (Taipei, Taiwan; approval no. A202215163).

Patient consent for publication

Informed consent was obtained from the patient for the publication of this case report, including the personal medical history and images without disclosing the patient's identity.

Competing interests

The authors declare that they have no competing interests.

References

1. Siegel RL, Miller KD, Fuchs HE and Jemal A: Cancer statistics, 2022. CA Cancer J Clin 72: 7-33, 2022.
2. Wu SJ, Huang SY, Lin CT, Lin YJ, Chang CJ and Tien HF: The incidence of chronic lymphocytic leukemia in Taiwan, 1986-2005: A distinct increasing trend with birth-cohort effect. Blood 116: 4430-4435, 2010.
3. Ko BS, Chen LJ, Huang HH, Chen HM and Hsiao FY: Epidemiology, treatment patterns and survival of chronic lymphocytic leukaemia/small lymphocytic lymphoma (CLL/SLL) in Taiwan, 2006-2015. Int J Clin Pract 75: e14258, 2021.
4. Raufi A, Alsharedi M, Khelfa Y, Griswold DC and Lebowicz Y: Leukemia cutis in a patient with chronic lymphocytic leukemia presenting as bilateral helical nodules. SAGE Open Med Case Rep 4: 2050313X16683624, 2016.
5. Hallek M, Cheson BD, Catovsky D, Caligaris-Cappio F, Dighiero G, Döhner H, Hillmen P, Keating M, Montserrat E, Chiorazzi N, *et al*: iwCLL guidelines for diagnosis, indications for treatment, response assessment, and supportive management of CLL. Blood 131: 2745-2760, 2018.
6. Van Dyke DL, Werner L, Rassenti LZ, Neuberg D, Ghia E, Heerema NA, Dal Cin P, Dell Aquila M, Sreekantaiah C, Greaves AW, *et al*: The Dohner fluorescence in situ hybridization prognostic classification of chronic lymphocytic leukaemia (CLL): The CLL Research Consortium experience. Br J Haematol 173: 105-113, 2016.
7. Michallet AS, Aktan M, Hiddemann W, Ilhan O, Johansson P, Laribi K, Meddeb B, Moreno C, Raposo J, Schuh A, *et al*: Rituximab plus bendamustine or chlorambucil for chronic lymphocytic leukemia: Primary analysis of the randomized, open-label MABLE study. Haematologica 103: 698-706, 2018.
8. Preetesh J, Michael JK, William GW, Mariela S, Philip AT, Alessandra F, Zeev E, Hagop K, Susan O and Jan AB: Long-term follow-up of treatment with ibrutinib and rituximab in patients with high-risk chronic lymphocytic leukemia. Clin Cancer Res 23: 2154-2158, 2017.
9. Meignan M, Gallamini A and Haioun C: Report on the first international workshop on interim-pet-scan in lymphoma. Leuk Lymphoma 50: 1257-1260, 2009.
10. Wagner G, Fenchel K, Back W, Schulz A and Sachse MM: Leukemia cutis-epidemiology, clinical presentation, and differential diagnoses. J Dtsch Dermatol Ge 10: 27-36, 2012.
11. Lazarian G, Munger M, Quinquenel A, Dilhuydy MS, Veronese L, Luque Paz D, Guièze R, Ledoux-Pilon A, Paillassa J, Merabet F, *et al:* Clinical and biological characteristics of leukemia cutis in chronic lymphocytic leukemia: A study of the French innovative leukemia organization (FILO). Am J Hematol 96: E353-E356, 2021.
12. Velez NF, Karia PS, Vartanov AR, Davids MS, Brown JR and Schmults CD: Association of advanced leukemic stage and skin cancer tumor stage with poor skin cancer outcomes in patients with chronic lymphocytic leukemia. JAMA Dermatol 150: 280-287, 2014.
13. Gao S, Shu H and Yang H: Imaging features of skeletal muscle lymphoma: A case report and literature review. BMC Med Imaging 21: 136, 2021.

14. Mollejo M and Piris MA: The complex pathology and differential diagnosis of splenic and nodal marginal zone lymphoma. Ann Lymphoma 4: 1-14. 2020.
15. Julie M Vose: Mantle cell lymphoma: 2017 update on diagnosis, risk-stratification, and clinical management. Am J Hematol 92: 806-813, 2017.
16. Cheson BD, Fisher RI, Barrington SF, Cavalli F, Schwartz LH, Zucca E, Lister TA; Alliance, Australasian Leukaemia and Lymphoma Group, Eastern Cooperative Oncology Group, *et al*: Recommendations for initial evaluation, staging, and response assessment of hodgkin and non-hodgkin lymphoma: The lugano classification. J Clin Oncol 32: 3059-3068, 2014.
17. National Comprehensive Cancer Network: Chronic Lymphocytic Leukemia/Small Lymphocytic Lymphoma (version 1.2024). https://www.nccn.org/professionals/physician_gls/pdf/cll_blocks.pdf
18. Maeshima AM, Taniguchi H, Fujino T, Saito Y, Ito Y, Hatta S, Yuda S, Makita S, Fukuhara S, Munakata W, *et al*: Immunohistochemical CD20-negative change in B-cell non-Hodgkin lymphomas after rituximab-containing therapy. Ann Hematol 99: 2141-2148, 2020.
19. Hiraga J, Tomita A, Sugimoto T, Shimada K, Ito M, Nakamura S, Kiyoi H, Kinoshita T and Naoe T: Down-regulation of CD20 expression in B-cell lymphoma cells after treatment with rituximab-containing combination chemotherapies: Its prevalence and clinical significance. Blood 113: 4885-4893, 2009.